

Electronic Supplementary Information (ESI) for

**Designing Lanthanide Coordination Nanoframeworks as X-ray Responsive Radiosensitizers for Efficient Cancer Therapy**

Hanjie Zhang,<sup>‡</sup> Kun Ye,<sup>‡</sup> Xiaoting Huang,<sup>‡</sup> Xia Lin, Li Ma\* and Tianfeng Chen\*

<sup>‡</sup> These authors contributed equally to this work.

*Department of Chemistry, and Guangdong Provincial Key Laboratory of Functional Supramolecular Coordination Materials and Applications, Jinan University, Guangzhou, 510632, China.*

*Email: chem\_mali@jnu.edu.cn (L. Ma), tchentf@jnu.edu.cn (T. Chen).*

<b>Experimental section</b> .....	S3
<b>Fig. S1</b> Hpbc ligand employing a bismonodenate coordination mode to connect with two different Ln <sup>3+</sup> ions and two nitrogen atoms coordinated to another one Ln <sup>3+</sup> ion. ....	S8
<b>Table S1</b> Complex crystallographic data of Dy(Hpbc) <sub>2</sub> Cl, Gd(Hpbc) <sub>2</sub> Cl and Eu(Hpbc) <sub>2</sub> Cl .	S8
.....	S8
<b>Fig. S2</b> TEM images of the frameworks after nanocrystallization (Dy(Hpbc) <sub>2</sub> Cl (a) and Gd(Hpbc) <sub>2</sub> Cl (b)). ....	S9
<b>Fig. S3</b> Infrared spectra of the Ln-based coordination frameworks Dy(Hpbc) <sub>2</sub> Cl, Gd(Hpbc) <sub>2</sub> Cl and Eu(Hpbc) <sub>2</sub> Cl.....	S9
<b>Table S2</b> Anti-tumor activity of the Ln-based coordination frameworks. ....	S10
<b>Fig. S4</b> Ln-based coordination frameworks Dy(Hpbc) <sub>2</sub> Cl(a), Gd(Hpbc) <sub>2</sub> Cl (b) and Eu(Hpbc) <sub>2</sub> Cl (c) and X-rays inhibit Hela cell activity in a concentration and dose-dependent manner, and the combined effect can achieve enhancement the inhibitory effect. ....	S10
<b>Fig. S5</b> Flow cytometry analysis of the effect of the Ln-based coordination frameworks on the cell cycle of Hela cells. ....	S11
<b>Fig. S6</b> The flow analysis results of the sensitization effect of the Ln-based coordination frameworks Dy(Hpbc) <sub>2</sub> Cl(a) and Gd(Hpbc) <sub>2</sub> Cl(b). ....	S11
<b>Table S3</b> Bond Lengths(Å) and Angles (deg) for Dy(Hpbc) <sub>2</sub> Cl. ....	S12
<b>Table S4</b> Bond Lengths(Å) and Angles (deg) for Gd(Hpbc) <sub>2</sub> Cl. ....	S13
<b>Table S5</b> Bond Lengths(Å) and Angles (deg) for Eu(Hpbc) <sub>2</sub> Cl. ....	S15
<b>Supporting References</b> .....	S18

## Experimental section

**Materials.** 3,4-Diaminobenzoic acid, 2-pyridine carboxaldehyde and Methyl violet, were purchased from Shanghai Aladin Reagent Company. All the chemicals and solvents were analytically pure. Thiazolyl blue tetrazolium bromide (MTT), propidium iodide (PI) and 1,3-Diphenylisobenzofuran (DPBF) were purchased from Sigma-Aldrich. All antibodies used in this study were purchased from Cell Signaling Technology (Beverly, MA). The water used in cellular experiments was ultrapure, supplied by a Milli-Q water purification system from Millipore. All radiation experiments were performed by Elekta Precise linear accelerator was provided by Wu Jing Zong Dui Hospital of Guangdong Province, Guangzhou, China.

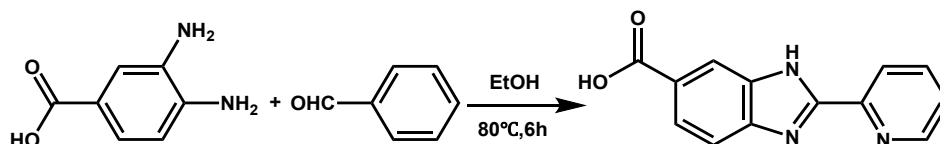
**Instruments.** Detection of single crystal structure of complexes were carried out on XtaLAB PRO X-ray single crystal diffractometer (Rigaku, Japan). The UV–Vis spectra of the compounds were obtained using the UH4150 UV–Visible (Hitachi, Japan). Infrared spectroscopy was characterized by Equinox 55 Fourier transform infrared spectroscopy (FT-IR) (Thermo Scientific, USA). Cell Viability analyzed by Cell Imaging Multi-Mode Reader (Bio Tek, USA). Cell cycle analysis was detected by Cyto FLEX Flow Cytometer (Beckman Coulter, USA).

**Crystallographic Studies.** Single crystal structures of Dy(Hpbc)<sub>2</sub>Cl, Gd(Hpbc)<sub>2</sub>Cl and Eu(Hpbc)<sub>2</sub>Cl were measured by X-ray diffraction. Data collection was performed on a High-Voltage Power Supply Diffractometer System equipped with a MicroMax-007DW MicroFocus X-ray generator and Pilatus 200K silicon diarray detector (Rigaku, Japan, Cu K $\alpha$ ,  $\lambda = 1.54184 \text{ \AA}$ ). Crystals were measured at 150 K. The structure was solved by direct methods and refined by full-matrix least-squares refinements based on F<sub>2</sub>. Anisotropic thermal parameters were applied to all non-hydrogen atoms. The hydrogen atoms were generated geometrically. The crystallographic calculations were performed using the SHELXL-2014/7 programs. The treatment for the disordered guest molecules in the cavities of all complexes involved the use of the SQUEEZE program of PLATON. Crystal data and structure refinement were summarized in Table S1-S4. CCDC NO: 1843166-1843168.

## Synthesis of complexes

### Synthesis of 2-(pyridin-2-yl)-1H-benzo[d]imidazole-6-carboxylic acid (H<sub>2</sub>pbcb) ligand.

The ligands were synthesized based on our previously reported synthesis method.<sup>1</sup> 3,4-Diaminobenzoic acid and 2-pyridinecarboxaldehyde (1:1, n: n) were added to ethanol, and refluxed at 80°C for 6 hours. The cooled reaction liquid was poured into pure water, and a pale yellow solid was precipitated. Filter and collect the filter residue to obtain the ligand.



**Scheme S1.** Synthesis of H<sub>2</sub>pbcb ligand.

**Synthesis of Dy(Hpbcb)<sub>2</sub>Cl.** H<sub>2</sub>pbcb and DyCl<sub>3</sub>(1:1, m:m) were dissolved in a mixed solution of water and acetonitrile. Then the reaction solution was transferred to a hydrothermal reactor with a polytetrafluoroethylene substrate, and reacted at 170°C for 48 h. Slowly cooled to room temperature, filtered and washed to obtain pale yellow lumpy crystals. Elemental analysis results show that the synthesized crystal material contains one molecule of crystal water, thus the molecular formula can be abbreviated as Dy(Hpbcb)<sub>2</sub>Cl • H<sub>2</sub>O. (Found: C, 44.17; H, 2.86; N, 11.67. Calc. for Dy(Hpbcb)<sub>2</sub>Cl • H<sub>2</sub>O: C, 43.96; H, 2.84; N, 11.83)

**Synthesis of Gd(Hpbcb)<sub>2</sub>Cl.** H<sub>2</sub>pbcb and GdCl<sub>3</sub>(1:1, m:m) were dissolved in a mixed solution of water and acetonitrile. Then the reaction solution was transferred to a hydrothermal reactor with a polytetrafluoroethylene substrate, and reacted at 170°C for 48 hours. Slowly cooled to room temperature, filtered and washed to obtain pale yellow lumpy crystals. Elemental analysis results show that the synthesized crystal material contains four molecule of crystal water, thus the molecular formula can be abbreviated as

Gd(Hpbcb)<sub>2</sub>Cl • 4H<sub>2</sub>O. (Found: C, 42.62; H, 2.93; N, 11.30. Calc. for Gd(Hpbcb)<sub>2</sub>Cl • 4H<sub>2</sub>O: C, 42.13; H, 3.26; N, 11.34)

**Synthesis of Eu(Hpbcb)<sub>2</sub>Cl.** H<sub>2</sub>pbcb and EuCl<sub>3</sub>(1:1, m:m) were dissolved in a mixed solution of water and acetonitrile. Then the reaction solution was transferred to a hydrothermal reactor with a polytetrafluoroethylene substrate, and reacted at 170°C for 48 hours. Slowly

cooled to room temperature, filtered and washed to obtain pale yellow lumpy crystals. Elemental analysis results show that the synthesized crystal material contains one molecule of crystal water, thus the molecular formula can be abbreviated as  $\text{Eu}(\text{Hpbc})_2\text{Cl} \cdot \text{H}_2\text{O}$ . (Found: C, 45.93; H, 3.18; N, 12.26. Calc. for  $\text{Eu}(\text{Hpbc})_2\text{Cl} \cdot \text{H}_2\text{O}$ : C, 45.80; H, 2.66; N, 12.33)

**Crystallographic Studies.** Single crystal structures of  $\text{Dy}(\text{Hpbc})_2\text{Cl}$ ,  $\text{Gd}(\text{Hpbc})_2\text{Cl}$  and  $\text{Eu}(\text{Hpbc})_2\text{Cl}$  were measured by X-ray diffraction. Data collection was performed on a High-Voltage Power Supply Diffractometer System equipped with a MicroMax-007DW MicroFocus X-ray generator and Pilatus 200K silicon diarray detector (Rigaku, Japan,  $\text{Cu K}\alpha$ ,  $\lambda = 1.54184 \text{ \AA}$ ). Crystals were measured at 150 K. The structure was solved by direct methods and refined by full-matrix least-squares refinements based on  $F^2$ . Anisotropic thermal parameters were applied to all non-hydrogen atoms. The hydrogen atoms were generated geometrically. The crystallographic calculations were performed using the SHELXL-2014/7 programs. The treatment for the disordered guest molecules in the cavities of all complexes involved the use of the SQUEEZE program of PLATON. Crystal data and structure refinement were summarized in Table S1-S4. CCDC NO: 1843166-1843168.

**Nanoization of  $\text{Dy}(\text{Hpbc})_2\text{Cl}$ ,  $\text{Gd}(\text{Hpbc})_2\text{Cl}$  and  $\text{Eu}(\text{Hpbc})_2\text{Cl}$  Complexes.** The obtained complexes were ground into a powder, and then dispersed in ultrapure water and ultrasonicated for 12 h. The suspension was collected by gradient centrifugation. Centrifuge at 2000 rpm for 5 minutes to remove large particles, followed by centrifugation at 8000 rpm for 15 minutes to obtain the complexes of small particles.

**Cell culture, MTT assay and determination of growth inhibition.** Cervical cancer cells (Hela, SiHa, Caski) and Ect1/E6E7 normal cervical cells were purchased from American Type Culture Collection (ATCC, Manassas, VA). All cells were cultured in DMEN with 10% FBS, penicillin (100 units/ml) and streptomycin (50 units/ml) at 37 °C in  $\text{CO}_2$  incubator (95% relative humidity, 5%  $\text{CO}_2$ ). The cell viability with and without radiation was examined by MTT assay.<sup>2</sup> Cells were seeded in 96-wells plate for 24 h (the density of cells are  $2 \times 10^4$ ), cultured with various doses of complexes for 72 h. After incubation, 30

μL per well of MTT solution (5 mg/ml) was added and then incubated for 4 further hours. Then, the medium was replaced with 150 μl DMSO per well. After 24 hours of incubation, the cells in the complex combined radiotherapy group were added with different concentrations of complexes and irradiated with different doses (0, 2 and 4 Gy) of X-rays. After incubating for 72 hours, cell viability analysis was performed by MTT method. The colour intensity of the solution, which reflects the cell growth condition, was measured at 570 nm by microplate spectrophotometer (Versamax).

Cell growth inhibition (%) =  $(OD_{\text{control}} - OD_{\text{treatment}} - OD_{\text{blank}}) / (OD_{\text{control}} - OD_{\text{blank}}) \times 100\%$ .

The half maximal inhibitory concentration (IC<sub>50</sub>) was obtained from the plot of growth (%) vs. complex concentrations.

**Flow cytometric analysis.** Cells were seeded in 60 mm dishes to culture for 24 h (the density of cells are  $4 \times 10^5$ ), then incubated with different concentrations of complexes. The complex combined with radiotherapy group received different doses (0, 2 and 4 Gy) of X-rays. After this, cells were incubated for further 48 h. Cells were trypsinized and washed with PBS, followed by fixing with 70% ethanol overnight at -20°C. The cells were centrifuged at 1500 rpm/min for 10 min to remove the supernatant and washed once with PBS. Then dye with PI at room temperature and avoid light for 1h. After filtering with a 400 mesh screen, cells were determined with Epics XL-MCL flow cytometer (Beckman Coulter, Miami, FL) to analyze cell cycle distribution. Afterwards, use Multicycle software (Phoenix Flow system, San Diego, CA).<sup>3</sup> The proportions of cells in the G0/G1, S and G2/M phases are expressed as DNA histograms. By quantifying the cell cycle, it was found that the cell cycle was blocked after treatment. Each experiment records 10,000 cells per sample.

**Measurement of intracellular reactive oxygen species (ROS) generation.** The 1,3-diphenylisobenzofuran (DPBF) probe was used to evaluate the antioxidant capacity of the drug. The cell density in the 96-well plate was  $2 \times 10^4$  cells per well. After 24 hours of incubation, different concentrations of lanthanide complexes were added to incubate for 6 hours, and a final concentration of 10 μM DPBF probe is added to incubate for 15 minutes.

The fluorescence intensity of DPBF (Ex=410 nm, Em=460 nm) was measured using cytation multifunctional fluorescence microplate reader.

**Clonogenic Assays.** HeLa cells were seeded in 6-well plates at a density of  $2 \times 10^3$  cells/mL, and 30  $\mu$ M of lanthanide complexes were added after 24 hours of incubation. After 6 hours of incubation, different doses (0, 2, 4 Gy) of X-ray radiation were applied, and then the incubation was continued for 8 days. After the colony formed, the medium was aspirated and washed with PBS to remove the medium. Stained the cells with 1 mL of 5 mg/mL methyl violet solution for 3 hours, removed the methyl violet solution, air dried, and took pictures.<sup>4,5</sup>

**Mitochondrial analysis.**  $4 \times 10^4$  cells were seeded in a 2 cm confocal dish, and 60  $\mu$ M Eu(Hpbc)<sub>2</sub>Cl was added after the cells adhered to the wall. After a total of 6h incubation, they were treated with 4 Gy X-ray. The cells were stained with Mito-Tracker Green and Hochess, and observed with a laser confocal microscope.

**Western blot analysis.** The expression level of cellular proteins was examined by western bolt analysis.<sup>2</sup> In briefly, cells were cultured with lysis buffer to extract total cellar protein. Concentration of protein was detected by BSA assay. After electrophoresis, protein were transferred to nitrocellulose membrane and then blocked with 5% nonfat milk for 1 h, followed by incubating with primary corresponding antibodies over night at 4°C. The membranes were then incubated with secondary antibodies for 1 h at room temperature and wash by TBST for three times. Protein bands were visualized on X-ray film using enhanced chemiluminescence detection regents (Kodak).  $\beta$ -actin was used to confirm the equal loading and transfer of proteins.

**Statistical Analysis.** All the tests in this essay were duplicated at least three times, as well as the experimental results were displayed as mean  $\pm$  standard deviation (mean  $\pm$  SD). Using double-tailed Student's t-test and one-way analysis of variance to analyze the differences of two groups or three or more groups respectively. There are statistically significant requirements  $P < 0.05$  (\*) and  $P < 0.01$  (\*\*).

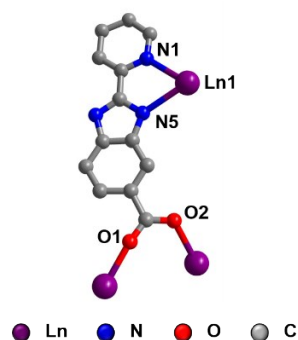


**Fig. S1** Hpbc ligand employing a bimonodenate coordination mode to connect with two different  $\text{Ln}^{3+}$  ions and two nitrogen atoms coordinated to another one  $\text{Ln}^{3+}$  ion; (b) Four Hpbc ligands link two adjacent  $\text{Ln}^{3+}$  ions through carboxylate group; (c) Three-dimensional structure of the framework. Purple: Ln; Gray: C; Blue: N; Red: O.

**Table S1** Complex crystallographic data of  $\text{Dy}(\text{Hpbc})_2\text{Cl}$ ,  $\text{Gd}(\text{Hpbc})_2\text{Cl}$  and  $\text{Eu}(\text{Hpbc})_2\text{Cl}$ .

Identification code	$\text{Dy}(\text{Hpbc})_2\text{Cl}$	$\text{Gd}(\text{Hpbc})_2\text{Cl}$	$\text{Eu}(\text{Hpbc})_2\text{Cl}$
Empirical formula	$\text{C}_{26}\text{H}_{16}\text{ClDyN}_6\text{O}_4$	$\text{C}_{26}\text{H}_{16}\text{ClGdN}_6\text{O}_4$	$\text{C}_{26}\text{H}_{15}\text{Cl}_2\text{EuN}_6\text{O}_4$
Formula weight	674.396	669.15	698.3
Temperature/K	150.00(10)	150.00(10)	150.00(10)
Crystal system	tetragonal	tetragonal	tetragonal
Space group	$I4_1/a$	$I4_1/a$	$I4_1/a$
$a/\text{\AA}$	16.32282(11)	16.35577(15)	16.32447(12)
$b/\text{\AA}$	16.32282(11)	16.35577(15)	16.32447(12)
$c/\text{\AA}$	22.3491(2)	22.4533(3)	22.3801(2)
$\alpha/^\circ$	90	90	90
$\beta/^\circ$	90	90	90
$\gamma/^\circ$	90	90	90
Volume/ $\text{\AA}^3$	5954.57(8)	6006.52(12)	5964.03(11)
$Z$	8	8	8
$\rho_{\text{calc}}/\text{g/cm}^3$	1.505	1.48	1.555
$\mu/\text{mm}^{-1}$	14.583	15.429	17.046
$F(000)$	2632	2616	2736
Crystal size/ $\text{mm}^3$	$0.2 \times 0.2 \times 0.2$	$0.15 \times 0.15 \times 0.12$	$0.15 \times 0.15 \times 0.15$

Radiation	CuK $\alpha$ ( $\lambda = 1.54184$ )	CuK $\alpha$ ( $\lambda = 1.54184$ )	CuK $\alpha$ ( $\lambda = 1.54184$ )
2 $\Theta$ range for data collection/ $^{\circ}$	12.76 to 148.28	6.68 to 148.04	6.702 to 148.24
Index ranges	-17 $\leq$ h $\leq$ 16, -20 $\leq$ k $\leq$ 16, -19 $\leq$ l $\leq$ 27	-19 $\leq$ h $\leq$ 20, -18 $\leq$ k $\leq$ 12, -24 $\leq$ l $\leq$ 27	-20 $\leq$ h $\leq$ 15, -18 $\leq$ k $\leq$ 19, -27 $\leq$ l $\leq$ 18
Reflections collected	8991	8930	8095
Independent reflections	3026 [ $R_{\text{int}} = 0.0224$ , $R_{\text{sigma}} = 0.0237$ ]	2980 [ $R_{\text{int}} = 0.0485$ , $R_{\text{sigma}} = 0.0378$ ]	2927 [ $R_{\text{int}} = 0.0336$ , $R_{\text{sigma}} = 0.0336$ ]
Data/restraints/parameters	3026/26/195	2980/30/177	2927/30/138
Goodness-of-fit on $F^2$	1.189	1.099	1.179
Final R indexes [ $I \geq 2\sigma(I)$ ]	$R_1 = 0.0391$ , $wR_2 = 0.0897$	$R_1 = 0.0661$ , $wR_2 = 0.1755$	$R_1 = 0.0826$ , $wR_2 = 0.1944$
Final R indexes [all data]	$R_1 = 0.0401$ , $wR_2 = 0.0901$	$R_1 = 0.0685$ , $wR_2 = 0.1773$	$R_1 = 0.0841$ , $wR_2 = 0.1949$
Largest diff. peak/hole / $e \text{ \AA}^{-3}$	0.52/-1.03	2.50/-2.30	1.32/-1.76

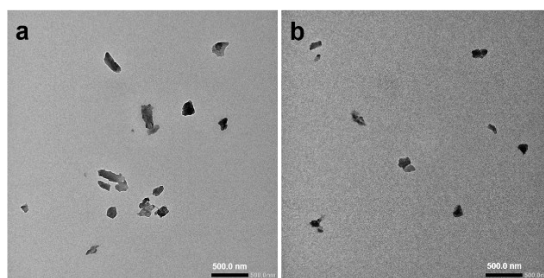


**Fig. S2** TEM images of the frameworks after nanocrystallization (Dy(Hpbc) $_2$ Cl (a) and Gd(Hpbc) $_2$ Cl (b)).

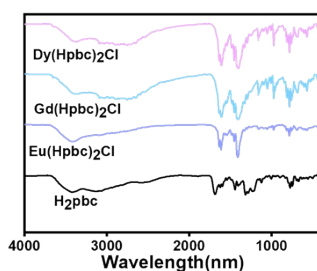


**Fig. S3** Infrared spectra of the Ln-based coordination frameworks Dy(Hpbc) $_2$ Cl, S9

Gd(Hpbc)<sub>2</sub>Cl and Eu(Hpbc)<sub>2</sub>Cl.

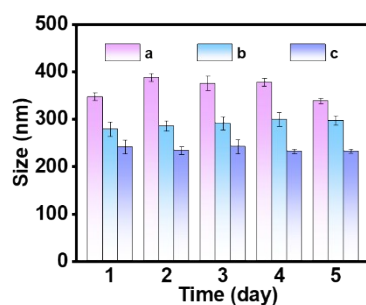


**Fig. S4** Dynamic light scattering characterizes the size of the Ln-based coordination frameworks(Dy(Hpbc)<sub>2</sub>Cl (a), Gd(Hpbc)<sub>2</sub>Cl (b) and Eu(Hpbc)<sub>2</sub>Cl (c)).

**Table S2** Anti-tumor activity of the Ln-based coordination frameworks.

Complexes	IC <sub>50</sub> (μM)					
	HeLa	SiHa	Caski	Ect1/E6E7	HeLa(with 2 Gy X-ray)	HeLa (with 4 Gy X-ray)
Dy(Hpbc) <sub>2</sub> Cl	45.13	27.86	40.67	24.69	31.42	22.64
Gd(Hpbc) <sub>2</sub> Cl	43.23	33.7	37.67	20.1	34.40	21.74
Eu(Hpbc) <sub>2</sub> Cl	43.06	28.59	26.84	16.52	33.00	20.84
Cisplatin	4.74	12.05	4.04	0.46	/	/

Safer Index =IC<sub>50</sub>(Ect1/E6E7)/IC<sub>50</sub>(Hela)=0.55, 0.47, 0.38, 0.10 for (Dy(Hpbc)<sub>2</sub>Cl, Gd(Hpbc)<sub>2</sub>Cl, Eu(Hpbc)<sub>2</sub>Cl and Cisplatin, respectively)

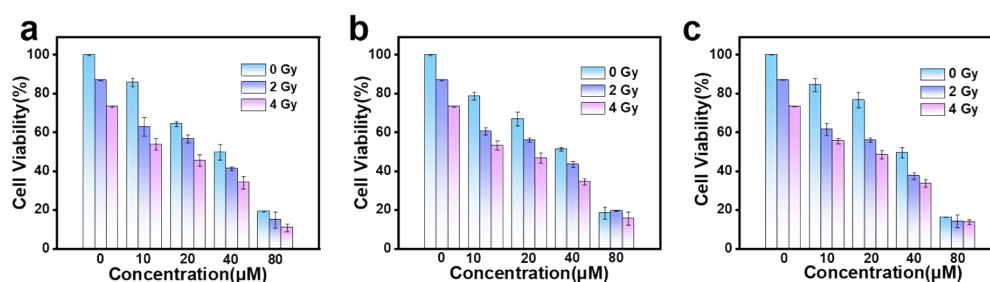


**Fig. S5** Ln-based coordination frameworks Dy(Hpbc)<sub>2</sub>Cl(a), Gd(Hpbc)<sub>2</sub>Cl (b) and Eu(Hpbc)<sub>2</sub>Cl (c) and X-rays inhibit Hela cell activity in a concentration and dose-dependent manner, and the combined effect can achieve enhancement the inhibitory effect. The cells were treated without/with radiotherapy 6 h after the Ln-based coordination frameworks were added, and incubated for 72 h after treatment.

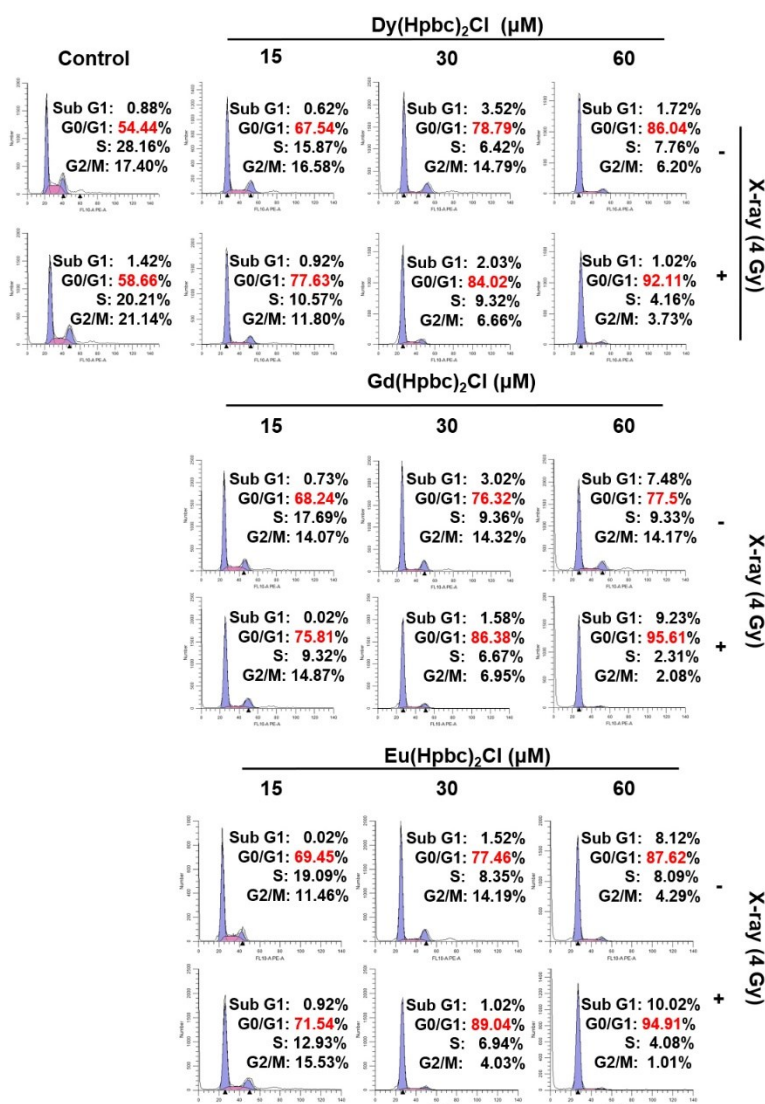


**Fig. S6** Flow cytometric analysis of the effect of the Ln-based coordination frameworks on the cell cycle of HeLa cells. The cells were treated without/with radiotherapy 6 h after the Ln-based coordination frameworks were added, and incubated for 48 h after treatment.

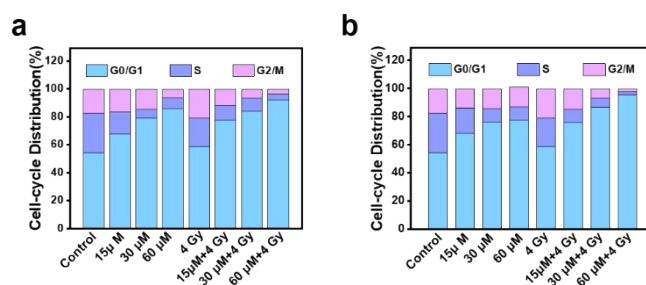


**Fig. S7** Flow cytometric analysis of the sensitization effect of the Ln-based coordination frameworks Gd(Hpbc)<sub>2</sub>Cl(a) and Eu(Hpbc)<sub>2</sub>Cl(b) on HeLa cells. The cells were treated without/with radiotherapy 6 h after the Ln-based coordination frameworks were added, and incubated for 48 h after treatment.

**Table S3** Bond Lengths(Å) and Angles (deg) for Dy(Hpbc)<sub>2</sub>Cl.

---

Dy1-N1 <sup>1</sup>	2.521(3)
Dy1-N1	2.521(3)
Dy1-N2 <sup>1</sup>	2.643(4)
Dy1-N2	2.643(4)
Dy1-O1 <sup>2</sup>	2.345(3)
Dy1-O1 <sup>3</sup>	2.345(3)
Dy1-O2 <sup>4</sup>	2.253(3)
Dy1-O2 <sup>5</sup>	2.253(3)
O1-Dy1 <sup>2</sup>	2.345(3)
O2-Dy1 <sup>6</sup>	2.253(3)
N1-Dy1-N1 <sup>1</sup>	74.06(17)
N1-Dy1-N2	63.35(12)
N1 <sup>1</sup> -Dy1-N2	77.09(12)
N1 <sup>1</sup> -Dy1-N2 <sup>1</sup>	63.35(12)
N1-Dy1-N2 <sup>1</sup>	77.09(12)
N2 <sup>1</sup> -Dy1-N2	130.21(16)
O1 <sup>2</sup> -Dy1-N1 <sup>1</sup>	133.88(11)
O1 <sup>2</sup> -Dy1-N1	80.25(11)
O1 <sup>3</sup> -Dy1-N1	133.88(11)
O1 <sup>3</sup> -Dy1-N1 <sup>1</sup>	80.25(11)
O1 <sup>2</sup> -Dy1-N2 <sup>1</sup>	74.04(12)
O1 <sup>2</sup> -Dy1-N2	123.44(12)
O1 <sup>3</sup> -Dy1-N2	74.04(12)
O1 <sup>3</sup> -Dy1-N2 <sup>1</sup>	123.44(12)
O1 <sup>2</sup> -Dy1-O1 <sup>3</sup>	141.70(14)
O2 <sup>4</sup> -Dy1-N1	102.02(12)
O2 <sup>5</sup> -Dy1-N1	143.66(12)
O2 <sup>4</sup> -Dy1-N1 <sup>1</sup>	143.66(12)
O2 <sup>5</sup> -Dy1-N1 <sup>1</sup>	102.02(12)
O2 <sup>4</sup> -Dy1-N2 <sup>1</sup>	152.35(12)

O2 <sup>5</sup> -Dy1-N2	152.35(12)
O2 <sup>5</sup> -Dy1-N2 <sup>1</sup>	69.44(12)
O2 <sup>4</sup> -Dy1-N2	69.44(12)
O2 <sup>4</sup> -Dy1-O1 <sup>2</sup>	78.56(12)
O2 <sup>5</sup> -Dy1-O1 <sup>3</sup>	78.56(12)
O2 <sup>5</sup> -Dy1-O1 <sup>2</sup>	77.39(12)
O2 <sup>4</sup> -Dy1-O1 <sup>3</sup>	77.39(12)
O2 <sup>4</sup> -Dy1-O2 <sup>5</sup>	101.17(16)
C1-N4-Dy1	134.4(3)
C2-N4-Dy1	117.6(3)
C3-N2-Dy1	124.1(3)
C4A-N2-Dy1	119.8(4)
C4B-N2-Dy1	115.2(11)
C5-O1-Dy1 <sup>2</sup>	120.7(3)
C5-O2-Dy1 <sup>6</sup>	160.4(3)

<sup>1</sup>1-X, 3/2-Y, +Z; <sup>2</sup>1-X, 1-Y, -Z; <sup>3</sup>+X, 1/2+Y, -Z; <sup>4</sup>1/4+Y, 5/4-X, 1/4+Z; <sup>5</sup>3/4-Y, 1/4+X, 1/4+Z; <sup>6</sup>5/4-Y, -1/4+X, -1/4+Z; <sup>7</sup>3/2-X, 3/2-Y, -1/2-Z.

**Table S4** Bond Lengths(Å) and Angles (deg) for Gd(Hpbc)<sub>2</sub>Cl.

Gd1-N2 <sup>1</sup>	2.549(6)
Gd1-N2	2.549(6)
Gd1-O1 <sup>2</sup>	2.296(5)
Gd1-O1 <sup>3</sup>	2.296(5)
Gd1-O2 <sup>4</sup>	2.372(5)
Gd1-O2 <sup>5</sup>	2.372(5)
Gd1-N1	2.669(6)
Gd1-N1 <sup>1</sup>	2.669(6)
O1-Gd1 <sup>6</sup>	2.296(5)
O2-Gd1 <sup>5</sup>	2.372(5)
N2-Gd1-N2 <sup>1</sup>	74.3(3)
N2-Gd1-N1 <sup>1</sup>	77.13(19)

N2 <sup>1</sup> -Gd1-N1 <sup>1</sup>	62.77(18)
N2 <sup>1</sup> -Gd1-N1	77.13(19)
N2-Gd1-N1	62.77(18)
O1 <sup>2</sup> -Gd1-N2 <sup>1</sup>	143.60(18)
O1 <sup>2</sup> -Gd1-N2	101.76(19)
O1 <sup>3</sup> -Gd1-N2	143.60(18)
O1 <sup>3</sup> -Gd1-N2 <sup>1</sup>	101.76(19)
O1 <sup>2</sup> -Gd1-O1 <sup>3</sup>	101.5(2)
O1 <sup>2</sup> -Gd1-O2 <sup>4</sup>	77.24(18)
O1 <sup>3</sup> -Gd1-O2 <sup>4</sup>	78.98(18)
O1 <sup>2</sup> -Gd1-O2 <sup>5</sup>	78.98(18)
O1 <sup>3</sup> -Gd1-O2 <sup>5</sup>	77.24(18)
O1 <sup>3</sup> -Gd1-N1 <sup>1</sup>	69.46(18)
O1 <sup>3</sup> -Gd1-N1	152.97(18)
O1 <sup>2</sup> -Gd1-N1	69.46(18)
O1 <sup>2</sup> -Gd1-N1 <sup>1</sup>	152.97(18)
O2 <sup>5</sup> -Gd1-N2	80.21(17)
O2 <sup>4</sup> -Gd1-N2	133.57(17)
O2 <sup>4</sup> -Gd1-N2 <sup>1</sup>	80.21(17)
O2 <sup>5</sup> -Gd1-N2 <sup>1</sup>	133.57(17)
O2 <sup>4</sup> -Gd1-O2 <sup>5</sup>	142.0(2)
O2 <sup>4</sup> -Gd1-N1 <sup>1</sup>	123.38(19)
O2 <sup>5</sup> -Gd1-N1 <sup>1</sup>	74.20(18)
O2 <sup>5</sup> -Gd1-N1	123.38(19)
O2 <sup>4</sup> -Gd1-N1	74.20(18)
N1-Gd1-N1 <sup>1</sup>	129.5(2)
C1-N2-Gd1	134.1(4)
C2-N2-Gd1	118.1(5)
C4AA-O1-Gd1 <sup>6</sup>	159.3(5)
C4AA-O2-Gd1 <sup>5</sup>	120.0(4)
C5-N1-Gd1	119.2(5)

C3-N1-Gd1 123.6(5)

<sup>1</sup>1-X, 3/2-Y, +Z; <sup>2</sup>3/4-Y, 1/4+X, 1/4+Z; <sup>3</sup>1/4+Y, 5/4-X, 1/4+Z; <sup>4</sup>+X, 1/2+Y, -Z; <sup>5</sup>1-X, 1-Y, -Z; <sup>6</sup>5/4-Y, -1/4+X, -1/4+Z; <sup>7</sup>1/2-X, 3/2-Y, -1/2-Z.

**Table S5** Bond Lengths(Å) and Angles (deg) for Eu(Hpbc)<sub>2</sub>Cl.

Eu1-O2 <sup>1</sup>	2.304(8)
Eu1-O2 <sup>2</sup>	2.304(8)
Eu1-O1 <sup>3</sup>	2.383(7)
Eu1-O1 <sup>4</sup>	2.383(7)
Eu1-N2	2.557(8)
Eu1-N2 <sup>5</sup>	2.557(8)
Eu1-N1 <sup>5</sup>	2.683(8)
Eu1-N1	2.683(8)
Eu1-C2 <sup>3</sup>	3.206(11)
Eu1-C2 <sup>4</sup>	3.206(11)
Eu1-Eu1 <sup>6</sup>	4.3981(14)
C2-Eu1 <sup>4</sup>	3.206(11)
O1-Eu1 <sup>4</sup>	2.383(7)
O2-Eu1 <sup>7</sup>	2.304(8)
O2 <sup>1</sup> -Eu1-O2 <sup>2</sup>	101.0(4)
O2 <sup>1</sup> -Eu1-O1 <sup>3</sup>	79.5(3)
O2 <sup>2</sup> -Eu1-O1 <sup>3</sup>	76.5(3)
O2 <sup>1</sup> -Eu1-O1 <sup>4</sup>	76.5(3)
O2 <sup>2</sup> -Eu1-O1 <sup>4</sup>	79.5(3)
O1 <sup>3</sup> -Eu1-O1 <sup>4</sup>	141.9(3)
O2 <sup>1</sup> -Eu1-N2	143.3(3)
O2 <sup>2</sup> -Eu1-N2	102.2(3)
O1 <sup>3</sup> -Eu1-N2	133.6(2)
O1 <sup>4</sup> -Eu1-N2	80.2(2)
O2 <sup>1</sup> -Eu1-N2 <sup>5</sup>	102.2(3)
O2 <sup>2</sup> -Eu1-N2 <sup>5</sup>	143.3(3)

O1 <sup>3</sup> -Eu1-N2 <sup>5</sup>	80.2(2)
O1 <sup>4</sup> -Eu1-N2 <sup>5</sup>	133.6(2)
N2-Eu1-N2 <sup>5</sup>	74.4(4)
O2 <sup>1</sup> -Eu1-N1 <sup>5</sup>	69.3(3)
O2 <sup>2</sup> -Eu1-N1 <sup>5</sup>	153.6(3)
O1 <sup>3</sup> -Eu1-N1 <sup>5</sup>	123.2(3)
O1 <sup>4</sup> -Eu1-N1 <sup>5</sup>	74.3(3)
N2-Eu1-N1 <sup>5</sup>	77.3(3)
N2 <sup>5</sup> -Eu1-N1 <sup>5</sup>	62.7(3)
O2 <sup>1</sup> -Eu1-N1	153.6(3)
O2 <sup>2</sup> -Eu1-N1	69.3(3)
O1 <sup>3</sup> -Eu1-N1	74.3(3)
O1 <sup>4</sup> -Eu1-N1	123.2(3)
N2-Eu1-N1	62.7(3)
N2 <sup>5</sup> -Eu1-N1	77.3(3)
N1 <sup>5</sup> -Eu1-N1	129.6(4)
O2 <sup>1</sup> -Eu1-C2 <sup>3</sup>	71.9(3)
O2 <sup>2</sup> -Eu1-C2 <sup>3</sup>	61.6(3)
O1 <sup>3</sup> -Eu1-C2 <sup>3</sup>	19.8(3)
O1 <sup>4</sup> -Eu1-C2 <sup>3</sup>	122.5(3)
N2-Eu1-C2 <sup>3</sup>	144.7(3)
N2 <sup>5</sup> -Eu1-C2 <sup>3</sup>	99.7(3)
N1 <sup>5</sup> -Eu1-C2 <sup>3</sup>	131.7(3)
N1-Eu1-C2 <sup>3</sup>	82.0(3)
O2 <sup>1</sup> -Eu1-C2 <sup>4</sup>	61.6(3)
O2 <sup>2</sup> -Eu1-C2 <sup>4</sup>	71.9(3)
O1 <sup>3</sup> -Eu1-C2 <sup>4</sup>	122.5(3)
O1 <sup>4</sup> -Eu1-C2 <sup>4</sup>	19.8(3)
N2-Eu1-C2 <sup>4</sup>	99.7(3)
N2 <sup>5</sup> -Eu1-C2 <sup>4</sup>	144.7(3)
N1 <sup>5</sup> -Eu1-C2 <sup>4</sup>	82.0(3)

N1-Eu1-C2 <sup>4</sup>	131.7(3)
C2 <sup>3</sup> -Eu1-C2 <sup>4</sup>	103.7(4)
O2 <sup>1</sup> -Eu1-Eu1 <sup>6</sup>	50.49(19)
O2 <sup>2</sup> -Eu1-Eu1 <sup>6</sup>	50.49(19)
O1 <sup>3</sup> -Eu1-Eu1 <sup>6</sup>	70.94(17)
O1 <sup>4</sup> -Eu1-Eu1 <sup>6</sup>	70.94(17)
N2-Eu1-Eu1 <sup>6</sup>	142.79(18)
N2 <sup>5</sup> -Eu1-Eu1 <sup>6</sup>	142.79(18)
N1 <sup>5</sup> -Eu1-Eu1 <sup>6</sup>	115.22(18)
N1-Eu1-Eu1 <sup>6</sup>	115.22(18)
C2 <sup>3</sup> -Eu1-Eu1 <sup>6</sup>	51.83(19)
C2 <sup>4</sup> -Eu1-Eu1 <sup>6</sup>	51.83(19)
C5-N2-Eu1	117.8(6)
C6AA-N2-Eu1	134.1(7)
C4-N1-Eu1	119.3(7)
C1-N1-Eu1	123.2(7)
O2-C2-Eu1 <sup>4</sup>	89.6(6)
O1-C2-Eu1 <sup>4</sup>	39.9(5)
C2-C2-Eu1 <sup>4</sup>	145.6(7)
C2-O1-Eu1 <sup>4</sup>	120.3(7)
C2-O2-Eu1 <sup>7</sup>	159.1(7)

---

<sup>1</sup>1/4+Y, 5/4-X, 1/4+Z; <sup>2</sup>3/4-Y, 1/4+X, 1/4+Z; <sup>3</sup>+X, 1/2+Y, -Z; <sup>4</sup>1-X, 1-Y, -Z; <sup>5</sup>1-X, 3/2-Y, +Z; <sup>6</sup>-1/4+Y, 5/4-X, 1/4-Z; <sup>7</sup>5/4-Y, -1/4+X, -1/4+Z; <sup>8</sup>1/2-X, 3/2-Y, -1/2-Z.

## References

- 1 Z. Zhao, P. Gao, Y. You, T. Chen, Cancer-Targeting Functionalization of Selenium-Containing Ruthenium Conjugate with Tumor Microenvironment-Responsive Property to Enhance Theranostic Effects, *Chem. Eur. J.*, 2018, **24**,3289-3298.
- 2 Z. Deng, L. Yu, W. Cao, W. Zheng, T. Chen, A selenium-containing ruthenium complex as a cancer radiosensitizer, rational design and the important role of ROS-mediated signalling, *Chem. Commun.*, 2015, **51**,2637-2640.
- 3 Y. Huang, L. He, W. Liu, C. Fan, W. Zheng, Y. Wong, T. Chen, Selective cellular uptake and induction of apoptosis of cancer-targeted selenium nanoparticles, *Biomaterials*, 2013, **34**,7106-7116.
- 4 L. He, H. Lai, T. Chen, Dual-function nanosystem for synergetic cancer chemo-/radiotherapy through ROS-mediated signaling pathways, *Biomaterials*, 2015, **51**,30-42.
- 5 D. Zeng, S. Deng, C. Sang, J. Zhao, T. Chen, Rational Design of Cancer-Targeted Selenadiazole Derivative as Efficient Radiosensitizer for Precise Cancer Therapy, *Bioconjugate Chem.*, 2018, **29**,2039-2049.